Section 5. Local Processes of Magnetic-Flux Emergence. Sunspot and Starspot Formation

https://doi.org/10.1017/S174392132400036X Published online by Cambridge University Press

Invited talks

https://doi.org/10.1017/S174392132400036X Published online by Cambridge University Press

Dynamics of Solar and Stellar Convection Zones and Atmospheres
Proceedings IAU Symposium No. 365, 2024
A. V. Getling & L. L. Kitchatinov, eds.
doi:10.1017/S174392132400036X

Signature of local (turbulent) dynamo on middle and small scales

V. I. Abramenko

Crimean Astrophysical Observatory of Russian Academy of Sciences, Nauchny, Russia
email: vabramenko@gmail.com

Abstract. The solar dynamo is a physical process of magnetic field generation due to conversion of kinetic energy of plasma flows into magnetic energy. However, in the mean-field dynamo theory, one needs to segregate scales and consider separately large-scale dynamo and small-scale dynamo. The large-scale dynamo produces the large-scale mean field and unavoidable fluctuations of the mean field. Both are cycle-dependent. The small-scale dynamo is supposed to produce only the small-scale field, and this field is cycle-independent. There is no sharp boundary between the intervals of the large-scale and small-scale dynamos. An unavoidable presence of a smooth transition implies that there is a region where the properties of the large-scale global dynamo and fluctuations inherent to small-scale dynamo co-exist on some intermediate scales. Recent achievements in observations of the small-scale dynamo operation on the smallest observable scales and on the intermediate scales of typical active regions are discussed in the review.

Keywords. Sun:magnetic fields, Sun:dynamo, turbulence

1. Introduction

The whole variety of observed solar magnetic fields is produced by the solar dynamo, which manifests itself differently on different scales. Although we know that there are no two absolutely similar solar cycles, yet, self-organization of the large-scale global dynamo remains impressive. In opposite, we observe a drastically different picture of chaos on smallest scales (the magnetic carpet), and something between chaos and order in the intermediate scales (typical active regions). Strictly speaking, the dynamo, as a physical process of magnetic field generation, has a unique underlying basis: conversion of kinetic energy of plasma flows into magnetic energy. In this sense, dynamo is a uniform mechanism. However, when we need to deal with a theoretical concept, say, the mean-field dynamo theory, we need to segregate scales and consider separately large-scale dynamo and small-scale dynamo. The large-scale dynamo produces the large-scale mean field and unavoidable fluctuations of the mean field. Both are cycle-dependent. The small-scale dynamo is supposed to produce only the small-scale field, and this field is cycle-independent. Of cause, there is no sharp boundary between the intervals of the large-scale and small-scale dynamos. An unavoidable presence of a smooth transition implies that there is a region where the properties of the large-scale global dynamo and fluctuations inherent to small-scale dynamo co-exist on some intermediate scales.

The helicity concept provides a specific view on the origin of the large-scale and small-scale dynamos. Depending on the presence or absence of the net flow helicity, two types of dynamo can be suggested, Meneguzzi *et al.* (1981). With the net helicity, magnetic energy grows on scales larger than the energy-containing scale of the fluid motions providing the

large-scale dynamo (LSD), or mean-field dynamo. The production of large-scale magnetic energy is ensured by the alpha-effect (see, e.g., Brandenburg (2003), Charbonneau (2020)).

Without the net helicity, the dynamo action is harder to achieve and the magnetic energy grows at scales smaller than the forcing scale. This process defines the small-scale dynamo (SSD), or the fluctuation dynamo Batchelor (1950), Kazantsev (1968), Petrovay and Szakaly (1993), Brandenburg and Subramanian (2005).

2. Small-Scale Dynamo (SSD)

Near the solar surface, the convective time scale is much shorter than the rotation period, therefore, the effects of rotation can be neglected, and a flow with no net helicity results. Any surface dynamo (local dynamo) will thus be the SSD.

Numerical simulations provide evidence of the SSD driven by turbulence at the solar surface (likely deeper as well). Since the pioneering publications by Petrovay and Szakaly (1993), and by Cattaneo (1999) a variety of approaches were suggested, for example, Vögler (and Schüssler2007), Pietarila Graham, Cameron, and Schüssler (2010), Rempel and Cheung (2014), Kitiashvili *et al.* (2015). Appearance of the magnetic filigree out of the seed field due to the turbulent convection is well proved from Figures 1 in works by Rempel and Cheung (2014) and Kitiashvili *et al.* (2015). The results of numerical simulations of SSD became more close to reality (as compared to the pioneering studies), embarrassing broader ranges as over the solar surface, so in depth and in height. The existence of the SSD is thought to be proved in numerical simulations.

Along with theoretical and numerical efforts, the observational studies of the small-scale magnetic features was continued. Thus, in the paper by Jin *et al.* (2011) on the basis of the MDI full disk data it was shown that the total (over the disk) unsigned magnetic flux from small-scale magnetic elements does not depend on the solar cycle. The authors applied the magnetic flux density of 15 Mx cm^{-2} as a threshold to outline active regions and then to segregate the quiet-sun flux from the active regions flux, see Figure 2 in Jin *et al.* (2011). This experiment clearly separates the total solar magnetic flux into: i) the cycle-dependent component, associated with active regions and caused presumably by the large-scale dynamo, and ii) the cycle independent component produced presumably by the small-scale local dynamo. The weak but still noticeable enhancement of the quiet-sun flux during the solar maximum might indicate a presence of the mean-field fluctuations in the small-scale flux.

Another similar experiment was undertaken by Obridko, Livshits, and Sokoloff (2017) on the basis of the same MDI data but another flux segregation criteria. The authors used three thresholds: 33, 100, and 3000 Mx cm^{-2}. The total unsigned flux from all pixels below a threshold was calculated (see Figure 3 in Obridko, Livshits, and Sokoloff (2017)). The lowest threshold data show no dependence on the cycle, the one-hundred threshold data show a very weak enhancement during the cycle maximum, and the 3000-threshold data actually correspond to the total flux from the entire disk and follow the cycle. So, the stronger the field, the more strong is the connection with the global dynamo. Thus, the authors concluded that the weak field of magnitude less than 100 Mx cm^{-2} apparently arise as a result of a small-scale sub-surface process, while the stronger fields are connected with the cycle and are generated by the classical mean-field solar dynamo.

3. Magnetic Power Spectra as a Tool to Diagnose SSD

However, the cycle-independence *per se* does not allow us to decide whether the observed effect is due to real field generation (SSD), or it is purely a result of turbulence, of direct turbulent cascade, as it is argued by Stenflo and Kosovichev (2012).

https://doi.org/10.1017/S174392132400036X Published online by Cambridge University Press

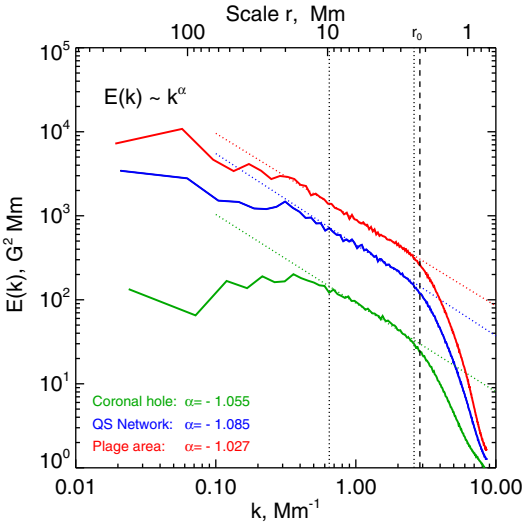

Figure 1. Magnetic power spectra calculated from three areas on the solar disk outside active regions. The full disk HMI/LOS magnetograms (hmi.M_720s series) taken on 10 February 2015 (Schou *et al.* (2012)) were used. The linear inertial range of (2.4-10) Mm is marked by the vertical dotted segments, and the scale r_0 corresponding to the triple resolution of HMI, is indicated with the vertical dashed line. The spectral indexes, α, derived from the best linear fit to the data points inside the inertial range, are listed in the lower left corner of the graph.

An analysis of the magnetic energy spectrum can help in this question. According to the classical turbulence theory by Kolmogorov (1941) (K41 theory), the energy input occurs at large scales and energy cascades down toward smallest scales so that the index of the power spectrum is -5/3. The cascade works as shredding and fragmentation of eddies. In this case, no additional energy input in intermediate scales is happen. The total amount of energy on small scales is assumed to originate from the direct turbulent cascade. However, in the case of additional energy input on some interval of scales due to some process, for example, the turbulent dynamo action, this energy becomes transferred up and down along the spectrum, the energy peak becomes smoothed and, as a result, the spectrum becomes more shallow than -5/3. So, the shape and slope of the magnetic power spectrum can tell us whether we deal with the turbulent cascade along, or some other processes are involved into the formation of the magnetic elements.

The magnetic power spectra determined from the SDO/HMI/LOS magnetograms for a coronal hole, a quiet sun, and a plage areas (Figure 1) exhibit the same spectral index of -1 on a broad range of spatial scales from 1020 Mm down to 2.4 Mm Abramenko and Yurchyshyn (2020). This implies that the same mechanism(s) of magnetic field generation operate everywhere in the undisturbed photosphere, and this mechanism is not the direct turbulent cascade only. The most plausible additional mechanism is the local turbulent dynamo. The similar inference on the basis of Hinode data was reported by other authors, for example, Ishikawa and Tsuneta (2010), Jin and Wang (2015).

To estimate qualitatively the productivity of the local small-scale dynamo, one needs to compare the magnetic spectra from the data obtained simultaneously by different instruments from the same area on the solar disk. On June 19, 2017 the Goode Solar Telescope at Big Bear Solar observatory, using the instrument Near InfraRed Imaging Spectrapolarimeter (NIRIS, Cao *et al.* (2012)), recorded a quiet-sun area on the disk center. A set of LOS magnetograms with the spatial resolution of 0.08 arcsec per pixel was acquired and used to calculate the average magnetic power spectrum (red line in

https://doi.org/10.1017/S174392132400036X Published online by Cambridge University Press

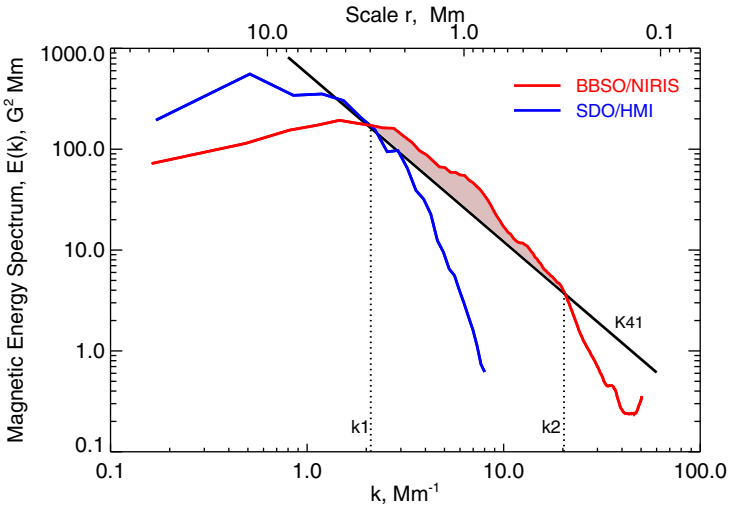

Figure 2. HMI (blue) and NIRIS (red) magnetic power spectra calculated over the same area of the solar photosphere. The black solid line shows the Kolmogorov-type K41 spectrum with the slope of -5/3. The shaded area shows the excess of magnetic energy above the K41 line within the $k_1 - k_2$ interval, which contains about 35% of the NIRIS energy in this interval.

Figure 2). Simultaneous maps of the LOS-field measured by HMI in the same area were used to derive the counterpart HMI-spectrum for comparison (blue line in Figure 2). If we consider an idea that following the K41 theory energy cascades from large scales (in this case, from scales of 3–5 Mm) down to small spatial scales, then the NIRIS spectrum should follow the K41 line (black solid line in Figure 2). However, within the interval between k_1 and k_2 the observed spectrum is well above the K41 line, which implies that besides the energy cascading to smaller scales along the inertial interval, an additional energy may be injected in this spectral range. Our estimates (Abramenko and Yurchyshyn (2020)) showed that the energy excess constitutes about 35% of the total NIRIS energy concentrated within the interval of (3.5 - 0.3) Mm. We emphasis that this is only a lower estimate of the energy excess because the high-frequency part of the spectrum is definitely lowered on the plot due to instrumental issues.

Comparison of magnetic spectra in quiet sun derived from different instruments (Abramenko, Yurchyshyn, and Goode (2012)) demonstrated that the spectrum tends to extent to the small-scale end as the resolution of an instrument improves (Figure 3). The spectrum from Nakagawa and Priest (1973) (black line), obtained from low-resolution Kit Peak data, shows only the energy on super-granula scales; the MDI spectrum (green line) shows the narrow inertial range with a slope close to -1 on scales around 10 Mm, the HMI spectrum follows with the same slope down to 4 Mm, and the Hinode spectra follow with the same slope down to 1 Mm. The spectrum, which is more shallow than the Kolmogorov -5/3 spectrum (the dashed K41 line), seems to be met on all observable scales.

Thus, in the entire undisturbed photosphere, the small-scale dynamo produces a substantial part of the total magnetic energy. The rest is presumably supplied by turbulent cascading of large-scale fields generated by the global dynamo.

4. Fluctuation Dynamo on Intermediate Scales

As mentioned in Introduction and argued by Stenflo and Kosovichev (2012), there exists no sharp transition between the global dynamo and SSD. Therefore, there should

https://doi.org/10.1017/S174392132400036X Published online by Cambridge University Press

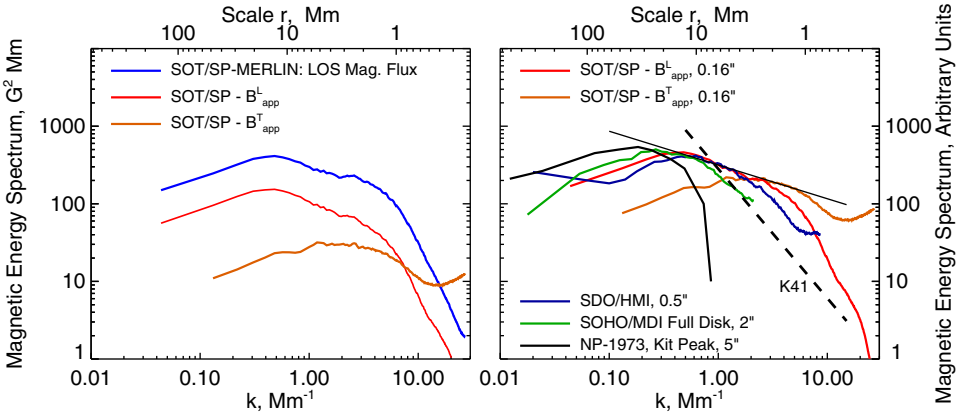

Figure 3. Magnetic energy spectra from quiet sun magnetograms obtained with different instruments. For better comparison, in the right panel the spectra are shifted along the vertical axis. Black line: Nakagawa and Priest (1973) spectrum. As the resolution improves, the cut-off of the spectra shifts toward the higher wave-numbers. The thin straight line shows a tentative behavior of the spectra as the resolution improves. The Kolmogorov spectrum with the slope of -5/3 is shown with the dashed line K41.

exist certain processes that introduce chaos on intermediate scales, for example, on the typical scales of active regions.

In general, there exists a possibility for the fluctuation dynamo to operate on typical scales of active regions (e.g., Brandenburg and Subramanian (2005), Sokoloff, Khlystova, and Abramenko (2015)). Continuous turbulence in the convection zone might affect the coherent toroidal field while it rises to the surface. Namely, the turbulence can distort the toroidal flux tubes and, even more, it can generate the additional flux. To explore the contribution of these processes, one has to segregate fluxes from active regions produced by the coherent global toroidal field (regular ARs), on one hand, and fluxes from active regions that were distorted by sub-photospheric turbulence (irregular, or complex ARs). Motivated by this reasoning, a new classification of active regions was suggested in Abramenko (2021). In brief, the underlying arguments to elaborate the magneto-morphological classification (MMC) were as follows.

A majority of active regions of all sizes are bipolar active regions and they follow the empirical laws, compatible with the mean-field dynamo theory, namely, the Hale polarity law, the Joy's law, and the rule of the leading sunspot prevalence (e.g., Babcock (1961), van Driel–Gesztelyi, Green (2015)). In the MMC, these active regions are classified as A-class, or regular active regions. Two sub-classes A1 and A2 were introduced to segregate in the A2-class those active regions, which contain a small (as compered to the leading sunspot) δ-structure. Scanty unipolar active regions were segregated to the separate class U. All the rest belong to the class of irregular active regions, B-class. Active regions of this class were also separated between three sub-classes: B1, B2, and B3. The sub-class B1 contains the wrong bipolar active regions, those violating at least one of the aforementioned empirical laws (emergence of a single toroidal flux tube rotated and/or inclined owing to the turbulent dynamo action); B2 - multipolar active regions consisting of several co-aligned bipoles (as a result of fragmentation and distortion of a single flux tube), or tight strong δ-structure (as a result of strong twist of a single flux tube by the turbulent dynamo action); B3 - multipolar ARs with chaotically distributed spots of both polarities (emergence of several intertwined by turbulent dynamo flux tubes). Examples of active regions of the A1-class (NOAA 12674) and of the B3-class (NOAA 12673) are shown in Figure 4.

https://doi.org/10.1017/S174392132400036X Published online by Cambridge University Press

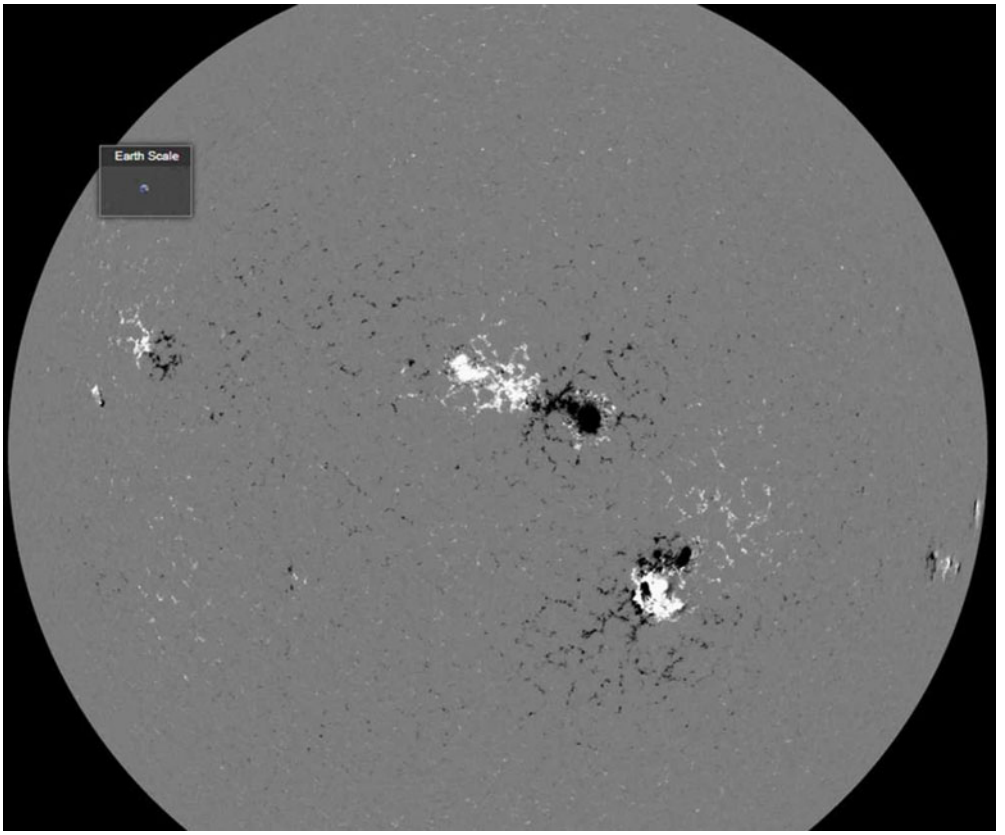

Figure 4. Examples of active regions of different magneto-morphological classes. In the Northern hemisphere the NOAA AR 12674 is observed: a bipolar magnetic structure complying with the Hale polarity lay, having the tilt angle in accordance with the Joy's law, and having the dominating leading sunspot; this active region belongs to the A1 class. In the Southern hemisphere the NOAA AR 12673 is observed: a multipolar structure with chaotically distributed sunspots; this active region was classified as B3-class active region.

In Abramenko *et. al* (2023) a set of independent snapshots of the solar disk magnetograms was compiled an utilized to explore how the summed (over the disk) magnetic flux from active regions of a given MMC class varies during the Solar Cycles 23 and 24. This experiment (see Figure 5) allowed the authors to reveal how the turbulent component of the dynamo manifests itself on the intermediate scales. It was found that the overall shape of the cycle is better correlated with the flux from all regular active regions, whereas the fine structure of the solar maximum (in particular, the origin of the secondary peaks in 2002 and 2014) is determined by the irregular active regions. Note also that the extreme flaring is caused by the active regions of B2 and B3 classes, Abramenko (2021).

During the phase of solar activity maximum, about a half of the total flux comes from irregular ARs and about the same amount comes from regular ARs, see Figure 5). So, about a half of the active regions flux is *distorted* by turbulence, however, not necessary *generated* by turbulence, because there exists (Abramenko *et. al* (2023)) a high correlation of the both fluxes with the cycle (the correlation coefficient CC between the A1+A2 (B1+B2+B3) and the total flux consists of 0.98 (0.94)) and between each other (CC between the A1+A2 and B1+B2+B3 fluxes consists of 0.88). This implies that the regular and irregular fluxes have a common origin: the coherent toroidal magnetic field generated by the global dynamo.

https://doi.org/10.1017/S174392132400036X Published online by Cambridge University Press

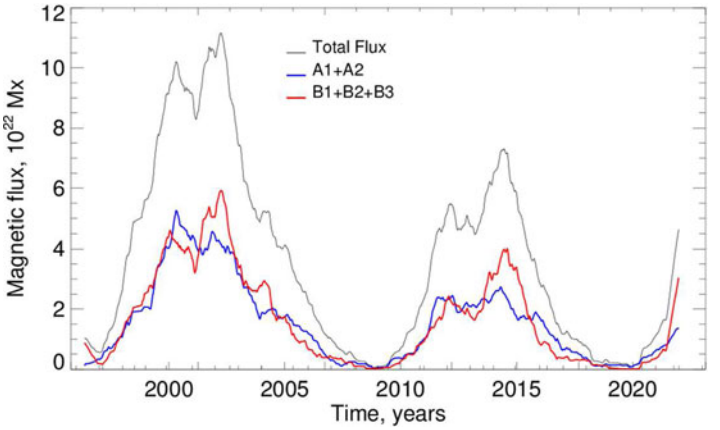

Figure 5. Time variations of the summed over the disk fluxes of active regions belonging to different MMC classes. Blue - fluxes of regular active regions (summed flux from A1 and A2 classes); red - fluxes of all irregular active regions (summed flux from B1, B2, and B3 classes). The thin black line shows the total over the disk flux from all active regions, including unipolar sunspots.

The deepest solar minima occur simultaneously for all classes. Moreover, during the minima, the irregular ARs are much more scanty than regular ones (see Suleymanova and Abramenko, this issue). So, the active regions generation during the solar minima is dominated by the global dynamo action with minor influence of the turbulence in the convection zone.

Therefore, a reservoir for all active regions' magnetic flux is the cycle-dependent global dynamo, whereas the turbulent convection hardly generates much flux, distorting a half of this flux during the active phase of a solar cycle.

5. Concluding Remarks

In summary, a manifestation of the local (small-scale, turbulent, or fluctuation) dynamo from the observational standpoint can be formulated as follows.

On the intra-network and network scales, the small-scale (local) dynamo is at work and generates more than 35% of the total magnetic energy, augmenting the direct turbulent cascade.

On intermediate scales of typical active regions, the solar dynamo operates as a unique process and generates ARs of all classes, whereas the turbulent component of dynamo (local dynamo) distorts a half of the emerging toroidal flux, determines the fine structure of the time profile of a cycle during a cycle maximum, causes the extreme flaring.

However, it would be very useful to keep in mind that from the physical standpoint, the segregation of the process of the magnetic flux generation into global (large-scale) dynamo and local (small-scale, turbulent, fluctuation) dynamo is very relative.

References

Abramenko, V., Yurchyshyn, V., and Goode, P.R. 2012, *4th Hinode Science Meeting: Unsolved Problems and Recent Insights*, 455, 17.
Abramenko, V.I. 2021, *MNRAS*, 507, 3698.
Abramenko, V.I. and Yurchyshyn, V.B.: 2020, *MNRAS*, 497, 5405.
Abramenko, V.I., Suleymanova, R.A., Zhukova, A.V. 2023, *MNRAS*,518,, 4746.
Babcock, H.W. 1961, *A&A*, 133, 572.
Batchelor, G.K. 1950, RSPSA, 201,405.

https://doi.org/10.1017/S174392132400036X Published online by Cambridge University Press

Brandenburg, A. 2003, *Turbulence and Magnetic Fields in Astrophysics*, Edited by E. Falgarone, and T. Passot., *LNP*, 614, 402.
Brandenburg, A. and Subramanian, K. 2005, *Phys. Rep.*, 417, 1.
Cao, W., Goode, P.R., Ahn, K., Gorceix, N., Schmidt, W., and Lin, H. 2012, *Second ATST-EAST Meeting: Magnetic Fields from the Photosphere to the Corona*, 463, 291.
Cattaneo, F. 1999, *ApJ*, 515, L39.
Charbonneau, P. 2020, *LRSP*, 17, 4.
Ishikawa, R. and Tsuneta, S. 2010, *ApJ*, 718, L171.
Jin, C. and Wang, J.: 2015, *ApJ*, 806, 174.
Jin, C.L., Wang, J.X., Song, Q., and Zhao, H. 2011, *ApJ*, 731, 37.
Kazantsev, A.P. 1968, *JETP*, 26, 1031.
Kitiashvili, I.N., Kosovichev, A.G., Mansour, N.N., and Wray, A.A. 2015, *ApJ*, 809, 84.
Kolmogorov, A. 1941, *Akad Nauk SSSR Doklady*, 30, 301.
Meneguzzi, M., Frisch, U., and Pouquet, A. 1981, *Phys. Rev.*, 47, L1060.
Nakagawa, Y. and Priest, E.R. 1973, *ApJ*, 179, 949.
Obridko, V.N., Livshits, I.M., and Sokoloff, D.D. 2017, *MNRAS*, 472, 2575.
Petrovay, K. and Szakaly, G. 1993, *A&A*, 274, 543.
Pietarila Graham, J., Cameron, R., and Schüssler, M. 2010, *ApJ*, 714, 1606.
Rempel, M. 2014, *ApJ*, 789, 132.
Schou, J., Borrero, J.M., Norton, A.A., Tomczyk, S., Elmore, D., and Card, G.L. 2012, *SoPh*, 275, 327.
Sokoloff, D., Khlystova, A., and Abramenko, V. 2015, *MNRAS*, 451, 1522.
Stenflo, J.O. 2012, *A&A*, 541, A17.
van Driel–Gesztelyi, L., Green, L.M. 2015, *LRSP*,12, 1.
Vögler, A., Schüssler, M. 2007, *A&A*, 465, L43.

https://doi.org/10.1017/S174392132400036X Published online by Cambridge University Press